MOLECULAR AND CELLULAR BIOLOGY, Mar. 2011, p. 1110–1120 Vol. 31, No. 6
0270-7306/11/$12.00 doi:10.1128/MCB.00989-10

Therapeutic Levels of the Hydroxmethylglutaryl-Coenzyme A Reductase Inhibitor Lovastatin Activate Ras Signaling via Phospholipase D2▽

Kwang-jin Cho,[1] Michelle M. Hill,[2,3] Sravanthi Chigurupati,[1] Guangwei Du,[1] Robert G. Parton,[3] and John F. Hancock[1]*

Department of Integrative Biology and Pharmacology, The University of Texas Medical School—Houston, 6431 Fannin Street, Houston, Texas 77030[1]; The University of Queensland, Diamantina Institute, Woolloongabba, Queensland 4102, Australia[2]; and The University of Queensland, Institute for Molecular Bioscience, St Lucia, Queensland 4072, Australia[3]

Received 24 August 2010/Returned for modification 28 September 2010/Accepted 24 December 2010

Hydroxmethylglutaryl (HMG)-coenzyme A (CoA) reductase inhibitors (statins) lower serum cholesterol but exhibit pleiotropic biological effects that are difficult to ascribe solely to cholesterol depletion. Here, we investigated the effect of lovastatin on protein prenylation and cell signaling. We show that high concentrations (50 μM) of lovastatin inhibit Ras, Rho, and Rap prenylation but that therapeutic levels of lovastatin (50 nM to 500 nM) do not. In contrast, depletion of cellular cholesterol by therapeutic levels of lovastatin increased Ras GTP loading and mitogen-activated protein kinase (MAPK) activation in human umbilical vein endothelial cells and rodent fibroblasts. Elevated Ras signaling was not seen in statin-treated cells if cholesterol levels were maintained by supplementation. Activation of Ras-MAPK signaling was a consequence of, and dependent on, activation of phospholipase D2 (PLD2). Expression of dominant interfering PLD2 or biochemical inhibition of PLD2 abrogated Ras and MAPK activation induced by lovastatin. In contrast, ectopic expression of wild-type PLD2 enhanced Ras and MAPK activation in response to therapeutic levels of lovastatin. Statin-induced cholesterol depletion also modestly activated the epidermal growth factor receptor (EGFR), resulting in downregulation of EGFR expression. These results suggest that statins modulate key cell signaling pathways as a direct consequence of cholesterol depletion and identify the EGFR-PLD2-Ras-MAPK axis as an important statin target.

Hydroxmethylglutaryl (HMG)-coenzyme A (CoA) reductase inhibitors (statins) are widely used for the treatment of hypercholesterolemia (39). These drugs block the conversion of HMG-CoA to mevalonate, a rate-limiting step in the cholesterol biosynthesis pathway (15). In addition to the cholesterol-lowering effect, there is extensive evidence for additional clinical effects. Statins improve endothelial function, promote vascular relaxation, and inhibit platelet aggregation in part by driving increased synthesis of nitric oxide (NO) (36). Statins therefore correct the reduced synthesis, release, and activity of endothelium-derived NO observed in hypercholesterolemic patients (39). Statins also promote atherosclerotic plaque stability (58), have anti-inflammatory effects (3, 60), and are associated with a reduced risk of Alzheimer's disease (39). Nevertheless, it has been difficult to mechanistically link many of these beneficial clinical effects directly to reduced cellular and serum cholesterol levels.

One class of signaling molecules that has been identified as putative cholesterol-independent targets of statin action are prenylated small GTPases (16, 17, 39, 42). Ras and Rho GTPases act as molecular switches to regulate cell proliferation, differentiation, apoptosis, and cytoskeletal reorganization (26, 31). The biological activity of these GTPases requires farnesylation or geranylgeranylation of C-terminal CAAX motifs (where C is Cys, A is aliphatic amino acid, and X is Ser or Met in Ras or Leu in Rho) (27). High concentrations of statins have long been known to block Ras and Rho prenylation (27) by blocking production of mevalonate, a precursor of farnesyl and geranylgeranyl pyrophosphates used for protein prenylation (15). However, it is unclear whether the therapeutic levels of statins that are achieved in patients are sufficiently high to do so (38, 56).

The plasma membrane is a complex, dynamic, and laterally heterogeneous structure, which imposes nonrandom distributions on proteins across different types of transient, nanoscale domains (23, 55, 59). The assembly of signaling proteins, including Ras GTPases and epidermal growth factor receptor (EGFR), into specific nanodomains and nanoclusters is essential for high-fidelity signal transmission (2, 30, 50, 52, 59). The spatial organization of signaling complexes on the plasma membrane is driven by lipid-lipid, protein-lipid, and protein-protein interactions. In consequence, perturbation of the lipid structure of the plasma membrane, as occurs following cholesterol depletion, can directly dysregulate signal transduction (12, 26, 46, 50, 51, 54). Here, we investigate whether Ras prenylation is affected by therapeutic levels of lovastatin and explore more broadly the effect of statins on Ras signal transduction. We identify a novel effect of statins on Ras signaling that is directly related to cholesterol depletion and involves remodeling of the lipid structure of the plasma membrane.

MATERIALS AND METHODS

Plasmids and reagents. Green fluorescent protein (GFP)-tagged wild-type (WT) murine phospholipase D2 (mPLD2 WT) and GFP-tagged mPLD2 K758R,

* Corresponding author. Mailing address: Department of Integrative Biology and Pharmacology, The University of Texas Medical School—Houston, 6431 Fannin Street, Houston, TX 77030. Phone: (713) 500-7356. Fax: (713) 500-7444. E-mail: John.F.Hancock@uth.tmc.edu.

▽ Published ahead of print on 18 January 2011.

kindly provided by Mike Frohman (Stony Brook University, Stony Brook, NY), were subcloned into the pEF6/V5-His-TOPO plasmid (Invitrogen, Australia). Antibodies against extracellular signal-regulated kinase 2 (ERK2) (C-14) (no. sc-521), K-Ras2B (C-19) (no. sc-521), H-Ras (F235) (no. sc-29), and N-Ras (F155) (no. sc-31) were obtained from Santa Cruz Biotechnology (CA). Monoclonal antibodies anti-caveolin-1 (no. 610406), anti-Ras (no. 610001), and anti-Rho (no. 610990) were obtained from BD Transduction Laboratories (Lexington, KY). Rabbit phospho-p44/42 mitogen-activated protein kinase (MAPK) (ERK1/2) (Thr202/Tyr204) antibody (no. 9101), mouse phospho-p44/42 MAPK (ERK1/2) (E10) antibody (no. 9106), rabbit phospho-Akt (pAkt) (Ser473) antibody (no. 9271), rabbit Akt antibody (no. 9272), mouse anti-phospho-EGF receptor (Y1068) antibody (no. 2236), rabbit total EGF receptor antibody (no. 2232), and rabbit Rap1A/B (26B4) antibody (no. 2399) were from Cell Signaling Technology (Beverly, MA). Monoclonal anti-GFP (no. 11814460001) was from Roche. Tertiary butanol (no. 360538), lipoprotein-deficient serum (LPDS) (S5394), low-density lipoprotein (LDL) from human plasma (LDL cholesterol [LDL-C]) (L7914), lovastatin (M2147), and mevalonate (M4667) were purchased from Sigma Aldrich.

Preparation of active lovastatin. Lovastatin was converted to an active form as described previously (35). Briefly, inactive lovastatin was dissolved in warm (55°C) ethanol, to which 0.6 M NaOH and H_2O were added. The solution was incubated at room temperate for 30 min to complete the opening of the beta-lactone ring. The final lovastatin solution was adjusted to pH 8.0 with HCl and stored as a 10 mM stock at −20°C.

Cell culture. Baby hamster kidney (BHK) cells were maintained in Dulbecco's modified Eagle medium (DMEM) (Gibco) supplemented with 10% donor calf serum (DCS) and 2 mM L-glutamine. Human umbilical vein endothelial cells (HUVECs) (CRL 1730; ATCC) were maintained in Ham's F-12K medium (Gibco) supplemented with 10% fetal calf serum (FCS), 2 mM L-glutamine, 0.1 mg/ml heparin (Sigma Aldrich), and 0.03 mg/ml endothelial cell growth supplement (ECGS) (Sigma Aldrich). The passage numbers of HUVECs used in this study were 3 and 4. All cell lines were grown at 37°C at 5% CO_2. For cholesterol depletion experiments, DCS or FCS was replaced with LPDS, which was supplemented where indicated with purified LDL-C. To generate stable cell lines, BHK cells were transiently transfected with GFP-mPLD2 WT or GFP-mPLD2 K758R using Lipofectamine reagent (Invitrogen) according to the manufacturer's instructions. Following an overnight incubation, cells expressing the transfected protein were sorted using fluorescence-activated cell sorting (FACS) and maintained in BHK medium containing 1 mg/ml G418 (Geneticin; Sigma Aldrich).

Cholesterol assays. Total cellular cholesterol levels were measured using an Amplex Red cholesterol assay kit (A12216; Invitrogen) according to the manufacturer's instructions.

Subcellular fractionation and Ras processing assays. Subcellular fractionation into S100 and P100 fractions after hypotonic lysis was carried out as described previously (54). Triton X-114 (TX-114) partitioning was carried out exactly as described previously (22, 25). Lysates of cells were prepared in ice-cold, precondensed 1% TX-114 (dissolved in 25 mM Tris-Cl [pH 7.5], 150 mM NaCl), cleared by centrifugation, and warmed for 2 min at 37°C. Detergent and aqueous phases, containing hydrophobic and hydrophilic proteins, respectively, were separated by centrifugation and analyzed by quantitative Western blotting.

Western blotting. Cells were washed in cold phosphate-buffered saline (PBS) and subjected to detergent lysis in a buffer containing 50 mM Tris (pH 7.5), 75 mM NaCl, 25 mM NaF, 5 mM $MgCl_2$, 5 mM EGTA, 1 mM dithiothreitol, 100 μM $NaVO_4$, 1% Nonidet P40 plus protease inhibitors. SDS-PAGE and immunoblotting with the specified antibody were performed using 20 μg of each lysate. Signal was detected by enhanced chemiluminescence (SuperSignal; Pierce, Thermo Fisher Scientific, Rockford, IL) and imaged by FluorChemQ (Alpha Inotech, San Leandro, CA). Quantification of intensities was performed using FluorChemQ software.

Ras RBD pulldown assay. Ras-GTP levels were measured in a glutathione *S*-transferase (GST)-Ras binding domain (RBD) pulldown assay as described previously (54). Samples were analyzed by quantitative Western immunoblotting using pan-Ras or Ras isoform-specific antibodies.

PLD assays. To assay the requirement for phospholipase D (PLD) activity cells were incubated for 4 h in 1% (vol/vol) *n*-butanol or *t*-butanol. PLD normally carries out a transphosphatidylation reaction using water as an acceptor to generate phosphatidic acid (PA). The enzyme, however, has a strong preference (1,000-fold) for primary alcohols over water, leading to the generation of phosphatidyl alcohols. The generation of phosphatidic acid by PLD is therefore efficiently blocked in the presence of low concentrations of the primary alcohol *n*-butanol but is unaffected in the presence of the tertiary alcohol, *t*-butanol (34).

Metabolic labeling and phosphatidic acid assay by TLC. A modified version of a previously described method (63) was used. After 32 h of lovastatin treatment, BHK cells were labeled with [^{3}H]palmitate (2 mCi/ml) for a further 14 h in the continued presence of lovastatin. The labeling medium was then replaced with fresh medium containing lovastatin for 2 h. Cells were then harvested with ice-cold methanol and vortexed with chloroform. After incubation at room temperature for 15 min, H_2O was added, followed by centrifugation. Twenty microliters of the lower organic phase was used for scintillation counting to estimate the total labeled phospholipids. The remainder of the organic phase was dried by vacuum centrifugation and resuspended in chloroform-methanol (19:1) for spotting onto thin-layer chromatography (TLC) plates (no. 2855-821; Whatman LK5D). The plate was developed using the upper phase of a mixture of ethylacetate-2,2,4 trimethylpentane (isooctane)-acetic acid-H_2O (110:50:20:100). The position of PA was identified by the synthetic 3,4-dihydroxyphenylalanine (DOPA) standard (840875C; Avanti Polar Lipids, Inc.) after iodine staining. The plate treated with Enhance spray (6NE970C; PerkinElmer) was then incubated with an X-ray film at −80°C for 48 h, and the bands corresponding to the phosphatidic acid standard were cut out for scintillation counting.

RESULTS

Effects of lovastatin on cellular cholesterol levels. The clinical effect of statins in reducing cellular cholesterol is mediated by two mechanisms. First, statins have a major site of action in the liver, where the drug is subject to extensive first-pass metabolism. Reduction in cellular cholesterol synthesis elevates hepatocyte expression of the LDL receptor, leading to increased clearance of plasma LDL by the liver and a reduction in circulating LDL cholesterol (LDL-C) levels. Current clinical guidelines advocate statin dose escalation to reduce LDL-C levels to ≤70 mg/dl in high-risk patients and ≤100 mg/dl in all hypercholesterolemic patients (20, 57). Second, statins can also directly reduce endogenous cholesterol synthesis in all extrahepatic tissues.

To explore the signaling effects of statin-induced cholesterol depletion, BHK cells and HUVECs were chosen as model fibroblast and endothelial cell lines, respectively. Cells were cultured in medium containing 10% lipoprotein-deficient serum (LPDS) to mimic the reduced LDL-C level induced by statins. The plasma lovastatin levels 6 h after therapeutic doses of 40 to 200 mg are in the range of 50 to 250 nM (38); however, given that higher doses of statins may be prescribed, we evaluated cells treated with lovastatin in a concentration range of 50 to 500 nM to fully capture likely therapeutic levels.

Figure 1a and c show that a major reduction in cellular cholesterol is achieved by growth in LPDS (reflecting the hepatic effect of statin in reducing plasma LDL-C levels), but this is modestly supplemented by a direct effect on *de novo* synthesis within the target cell, leading to a further decline in cellular cholesterol. The cholesterol content of LPDS is very low, equivalent to ~3 mg/dl of LDL-C. Therefore, to more precisely model the clinical situation, we supplemented LPDS with purified human LDL-C to give levels of 240 mg/dl (high cholesterol level) and 100 mg/dl (normal) and reassayed cholesterol levels. Figure 1b and d show that BHK cells and HUVECs cultured in LPDS plus 240 mg/dl LDL-C closely mirrored the control cells grown in DCS and FCS, respectively, in exhibiting a high basal cellular cholesterol level with no significant decrease in the presence of statin. In contrast, cells cultured in LPDS plus 100 mg/dl LDL-C had significantly lower basal cholesterol levels than cells grown in DCS or LPDS plus LDL-C 240 mg/dl and showed a further 15 to 18% fall on culture in 300 to 500 nM lovastatin. In sum, Fig. 1a to d show

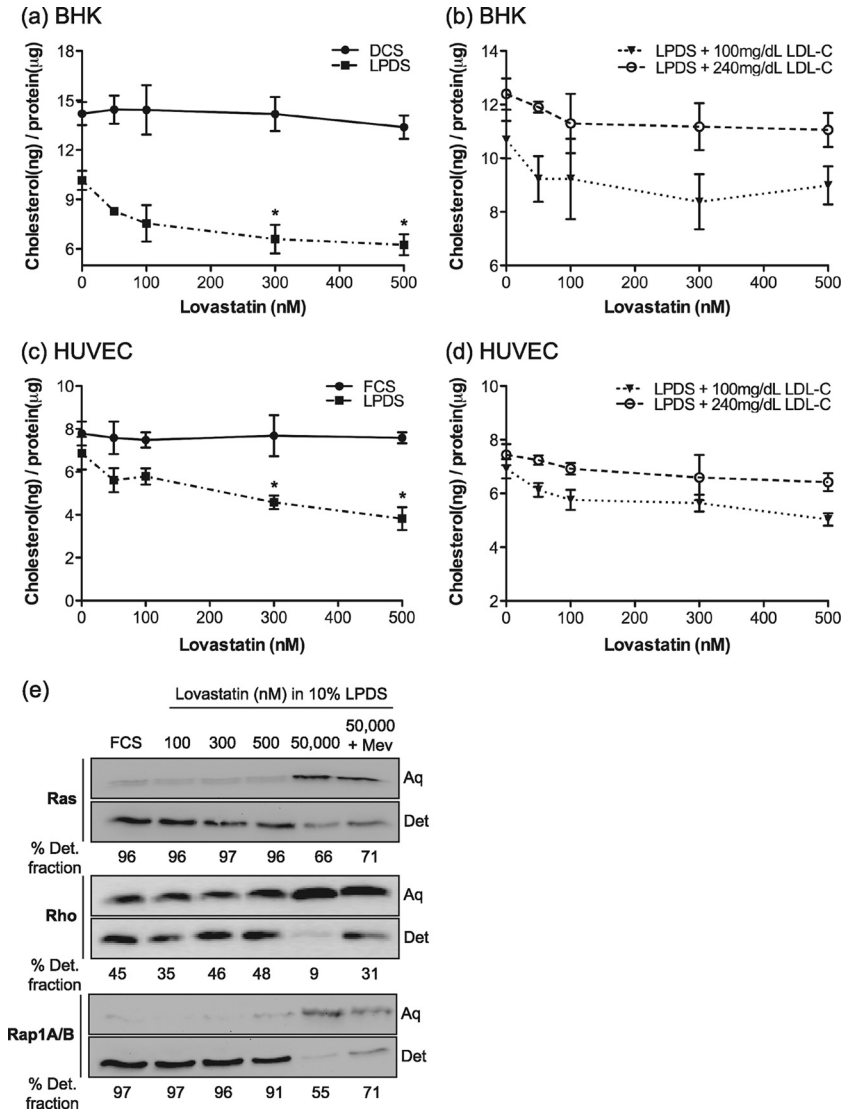

FIG. 1. Effect of therapeutic levels of lovastatin on cellular cholesterol and Ras prenylation. BHK cells (a) and HUVECs (c) were cultured in growth medium containing 10% DCS, 10% FCS, or 10% LPDS in the presence of lovastatin for 48 h. BHK cells (b) and HUVECs (d) were cultured in growth medium containing 10% LPDS supplemented with 100 or 240 mg/dl purified LDL-C. Total cellular cholesterol levels were measured. The graphs show means ± standard errors of the means (SEM) for 3 independent experiments. Differences between lovastatin-untreated and lovastatin-treated cells under each culture condition in panels a to d were assessed using one-way analysis-of-variance (ANOVA) tests, and significant differences are indicated (*, $P < 0.05$). (e) HUVECs were treated with various concentrations of lovastatin in the presence of 10% LPDS for 48 h. Control cells were cultured in standard growth medium containing 10% FCS. Cells were lysed in 1% Triton X-114 and lysates separated into detergent-enriched (Det.) and aqueous (Aq) phases by warming. After separation of the two phases by centrifugation, a 1× volume of the detergent-enriched phase (20 μl) containing hydrophobic proteins and a 2× volume of the aqueous phase (40 μl) containing hydrophilic proteins were blotted with an anti-pan Ras, anti-Rho, or anti-Rap1A/B antibody. A representative blot and mean percentages of the detergent fraction for 3 independent experiments are shown.

that an effect of statin on *de novo* cholesterol synthesis is observed only if the exogenous supply of cholesterol is substantially reduced by growth in LPDS with low LDL-C levels.

Effect of therapeutic levels of lovastatin on the prenylation of Ras and Rho GTPases. High concentrations of statins can prevent protein prenylation (37, 39, 53). To determine whether therapeutic levels of lovastatin inhibit prenylation of Ras and Rho GTPases, we examined steady-state levels of prenylated and nonprenylated Ras and Rho family proteins in lovastatin-treated cells by use of a Triton X-114 partitioning assay. This assay separates prenylated proteins from unprenylated proteins based on the increased hydrophobicity due to the farnesyl or geranylgeranyl anchor (22, 25, 27, 29). In control cells, the majority of endogenous Ras (farnesylated [6, 27]) and endogenous Rap1A/B (geranylgeranylated [4]) partitioned into the Triton X-114 detergent phase (Fig. 1e), and a substantial fraction of endogenous Rho (geranylgeranylated [1]) also partitioned into the detergent phase. The detergent fraction is lower because of the interaction of geranylgeranylated Rho with the chaperone protein RhoGDI (43). At all therapeutic

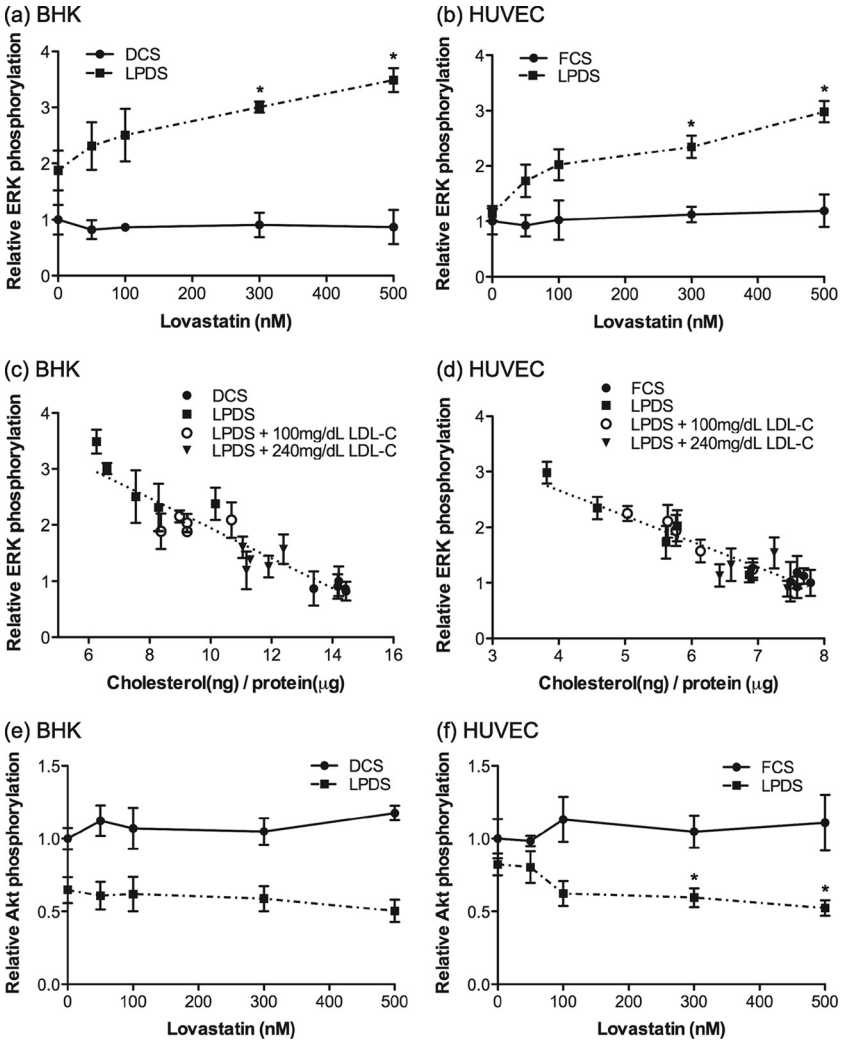

FIG. 2. Therapeutic levels of lovastatin modulate ERK and Akt activation. BHK cells (a and e) and HUVECs (b and f) were cultured in growth medium containing 10% DCS, 10% FCS, or 10% LPDS in the presence of lovastatin for 48 h. Cell lysates were assayed for ppERK or pAkt (S473) using phospho-specific antibodies and quantitative immunoblotting. The graphs show mean levels of ppERK or pAkt, relative to levels in cells grown in 10% DCS or FCS without lovastatin, ± SEM for 3 independent experiments. Differences between lovastatin-untreated and lovastatin-treated cells under each culture condition were assessed using one-way ANOVA tests, and significant differences are indicated (*, $P < 0.05$). (c and d) Total cellular cholesterol levels in Fig. 1 were plotted against the corresponding mean ppERK levels shown in panels a and b. The line was fitted by linear regression.

levels of lovastatin, the detergent partitioning of endogenous Ras, Rap, and Rho proteins was nearly identical to that in control cells, suggesting that protein prenylation was not affected at these concentrations. In the presence 50 μM lovastatin, however, the partitioning of endogenous Ras, Rho, and Rap into the aqueous phase of Triton X-114 significantly increased. The increased aqueous partitioning of Ras, Rho, and Rap was reversed when cells were supplemented with mevalonate, the direct product of HMG-CoA reductase. Subcellular fractionation also showed no reduction in binding of Ras to cellular membranes in cells grown in lovastatin concentrations of ≤500 nM (data not shown). Taken together, these results show that therapeutic levels of lovastatin have no significant effects on Ras, Rho, or Rap prenylation.

Cholesterol depletion by lovastatin activates Ras signaling. As therapeutic levels of lovastatin do not affect Ras prenylation, we investigated other mechanisms whereby lovastatin may modulate cellular signaling. We first examined activation of ERK and Akt as general screens for Ras signal output. Cells were treated with a range of concentrations of lovastatin in 10% LPDS for 48 h, and lysates were immunoblotted for phospho-ERK (ppERK) and phospho-Akt (pAkt). Control cells were grown in DCS or FCS with the same range of concentrations of lovastatin. In HUVECs and BHK cells, therapeutic levels of lovastatin in LPDS significantly increased the basal level of mitogen-activated protein kinase (MAPK) activity and reduced basal levels of pAkt (Fig. 2). A similar effect was also seen in cells grown in lovastatin in LPDS plus 100 mg/dl LDL-C (data not shown). Pooling the data sets from Fig. 1a to d with those of Fig. 2a and b reveals a striking inverse linear relationship between basal ppERK levels and cellular cholesterol content in both BHK cells and HUVECs (Fig. 2c and d).

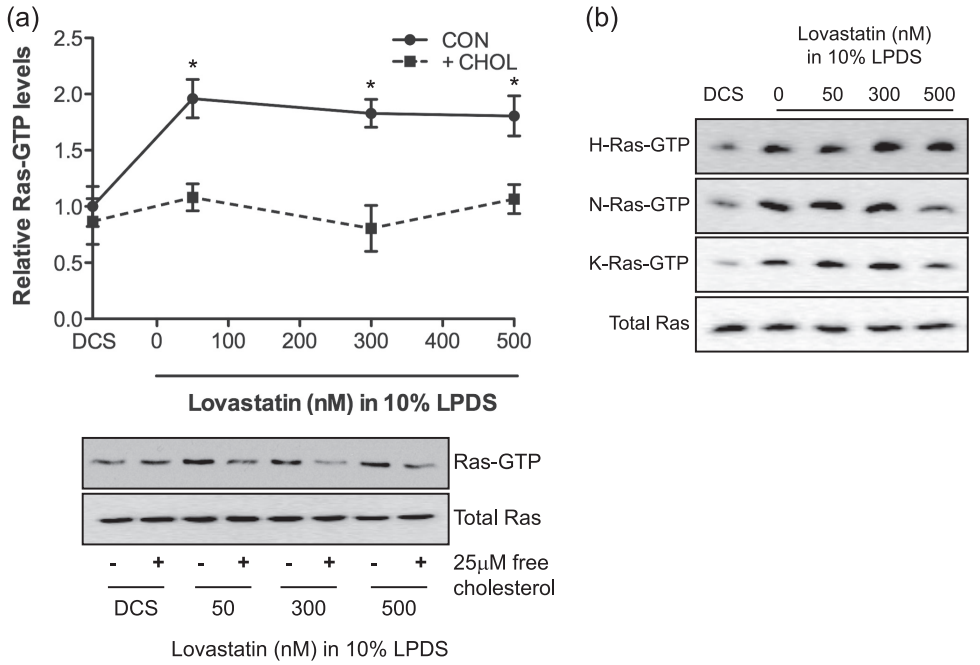

FIG. 3. Activation of Ras signaling by lovastatin is a consequence of cholesterol depletion. (a) BHK cells treated with lovastatin in the presence of 10% LPDS for 48 h were incubated with 25 μM water-soluble free cholesterol (+CHOL) or vehicle (CON) at 37°C for 20 min and harvested. Total Ras-GTP levels were measured in an RBD pulldown assay and compared to the level for cells grown in DCS. The graph shows mean fold increases in Ras-GTP levels ± SEM for 3 independent experiments. Differences between lovastatin-treated and control cells in the presence and absence of free cholesterol were assessed using one-way ANOVA tests. Significant differences are indicated (*, $P < 0.05$). A representative blot is shown. (b) BHK cells were treated with various concentrations of lovastatin in the presence of 10% LPDS for 48 h. Control cells were cultured in standard growth medium containing 10% DCS. H-, N-, and K-Ras-GTP loadings were measured using an RBD pulldown assay. A blot representative of 4 (H- and N-Ras) or 3 (K-Ras) independent experiments is shown.

To determine whether the increased MAPK activity was dependent on Ras activity, we directly measured Ras-GTP levels. These results showed that cholesterol depletion by therapeutic levels of lovastatin significantly activated Ras (Fig. 3a). Further analysis showed that all three Ras isoforms, H-, N-, and K-Ras, were activated (Fig. 3b). Similar effects of lovastatin were observed on acute Ras activation in response to serum stimulation (data not shown). The addition of water-soluble cholesterol to cells treated with therapeutic levels of lovastatin in 10% LPDS returned the elevated Ras GTP levels to control values (Fig. 3a). Similarly, BHK cells grown in DCS plus lovastatin, which did not show any elevation of MAPK activity or change in cellular cholesterol levels, did not exhibit elevated levels of Ras-GTP (Fig. 2 and data not shown). Taken together, these data suggest that elevated MAPK activity due to lovastatin-induced cholesterol depletion is a direct consequence of enhanced Ras activity and that activation of the Ras-MAPK pathway in cells chronically exposed to lovastatin correlates closely with cholesterol depletion.

Lovastatin-induced activation of Ras signaling is mediated by PLD2. We have shown that cholesterol depletion by therapeutic levels of lovastatin enhances Ras GTP loading, with a concomitant increase in ERK activation. Activation of the Ras-MAPK cascade could be at the level of receptors, such as the EGF receptor (EGFR), that couple to Ras, or the activity of RasGEFs or RasGAPs could be stimulated or inhibited, respectively. To discriminate between these possibilities, we examined the levels of EGFR and activated EGFR, monitored as Y1068 phospho-EGFR (2), in cells grown in LPDS with lovastatin. Figure 4a shows that total EGFR levels were significantly decreased after 48 h of growth in LPDS with lovastatin; however, the specific activity of the EGFR was simultaneously increased (Fig. 4b). In contrast, no change in EGFR levels was seen in cells grown in lovastatin and DCS rather than LPDS (Fig. 4c), conditions that do not change cellular cholesterol levels. Similar results were observed in HUVECs (data not shown).

Phospholipase D2 (PLD2), which is localized predominantly to the plasma membrane (10, 33, 34), hydrolyzes phosphatidylcholine to phosphatidic acid (34). Recent studies have shown that phosphatidic acid generated by PLD2 is an upstream regulator of Ras activation in EGF- and T-cell receptor-regulated signaling pathways (24, 45, 65). Following EGFR stimulation, phosphatidic acid produced by PLD2 recruits Sos to the plasma membrane, stimulating Ras activation. We therefore tested whether cholesterol depletion induced by lovastatin stimulates the catalytic activity of PLD2, leading to Ras and MAPK activation. BHK cells were treated with lovastatin for 44 h and then incubated in 1% primary (*n*)-butanol or tertiary (*t*)-butanol. Previous work has shown that *n*-butanol inhibits the production of phosphatidic acid by PLD but that *t*-butanol does not (45). Treatment with *n*- or *t*-butanol had no effect on Ras-GTP or ppERK levels in control cells. However, the elevated Ras-GTP and ppERK levels in cholesterol-depleted cells were significantly reduced after incubation in *n*-butanol but not after incubation in *t*-butanol (Fig. 5a and b).

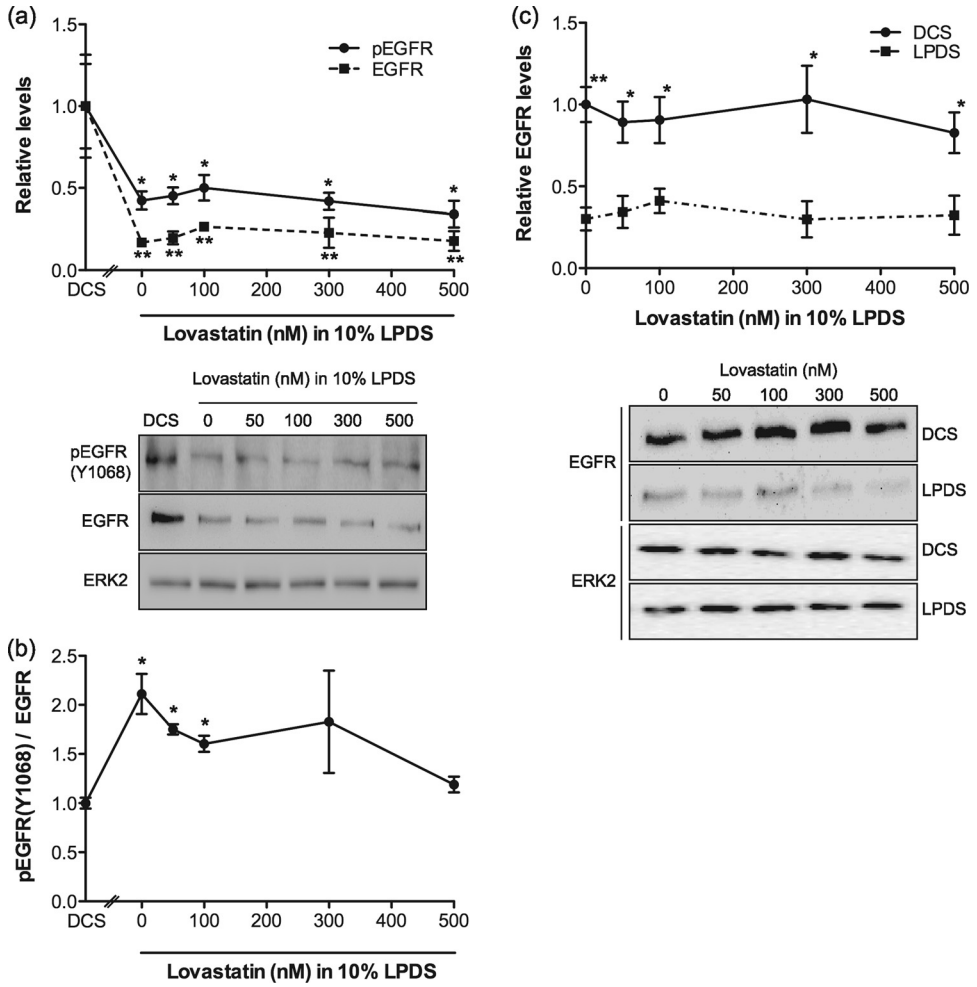

FIG. 4. EGF receptor expression is downregulated by lovastatin treatment. BHK cells were treated with lovastatin in the presence of 10% LPDS for 48 h. Control cells were cultured in standard growth medium containing 10% DCS. Total EGFR and phospho-EGFR (Y1068) levels were measured by quantitative immunoblotting. The graph in panel a shows mean EGFR and pEGFR levels ± SEM relative to levels in cells grown in control medium. An immunoblot representative of 3 independent experiments is also shown. ERK2 levels are used as a loading control. The specific activity of the EGFR (b) was estimated as the normalized ratio of phospho-EGFR to total EGFR using values obtained from panel a. For panels a and b, differences between lovastatin-treated and control cells were assessed using one-way ANOVA tests. Significant differences are indicated (*, $P < 0.05$; **, $P < 0.01$). (c) BHK cells were cultured in growth medium containing 10% DCS or 10% LPDS in the presence of lovastatin. Note that these growth conditions replicate those in Fig. 1a, where the presence of DCS maintains normal cell cholesterol levels in the presence of lovastatin. Total EGFR levels were measured by quantitative immunoblotting. The graph shows mean EGFR levels ± SEM relative to levels in cells grown in DCS. Differences between cells cultured in DCS and LPDS at each concentration of lovastatin were assessed using two-tailed *t* tests. Significant differences are indicated (*, $P < 0.05$; **, $P < 0.01$). An immunoblot representative of 3 independent experiments is also shown. ERK2 levels are used as a loading control.

If PLD activity is elevated as suggested by the data in Fig. 5, cells grown in LPDS and lovastatin would be expected to have elevated plasma membrane levels of phosphatidic acid compared to cells grown under control conditions. We first measured total cellular phosphatidic acid levels by metabolic labeling and thin-layer chromatography (63). Figure 6a shows that there is a dose-dependent increase in phosphatidic acid levels in cells grown in LPDS and increasing doses of lovastatin. To verify that plasma membrane levels of phosphatidic acid are specifically increased by lovastatin-induced cholesterol depletion, we made use of a previously characterized, fluorescent-tagged phosphatidic acid-binding probe (mGFP-NES-Spo20). Electron microscopy (EM) analysis of intact plasma membrane sheets prepared from BHK cells expressing mGFP-NES-Spo20 showed a significantly increased level of anti-GFP immunogold labeling after treatment for 48 h in lovastatin and LPDS (Fig. 6b). Increased phosphatidic acid production on the plasma membrane was further confirmed by increased fluorescence resonance energy transfer (FRET) between mGFP-NES-Spo20 and mRFP-NES-Spo20 in cells grown in lovastatin and LPDS (Fig. 6c).

Lovastatin-induced activations of PLD2 and EGFR are independent events. PLD2 is a downstream effector of the EGFR (45, 65); however, PLD2 activation also enhances EGFR clustering (2), which in turn might potentiate EGFR activation. We therefore explored the interplay between EGFR activation and PLD2 activation in cholesterol-depleted cells. Figure 7a shows that EGFR downregulation in lovasta-

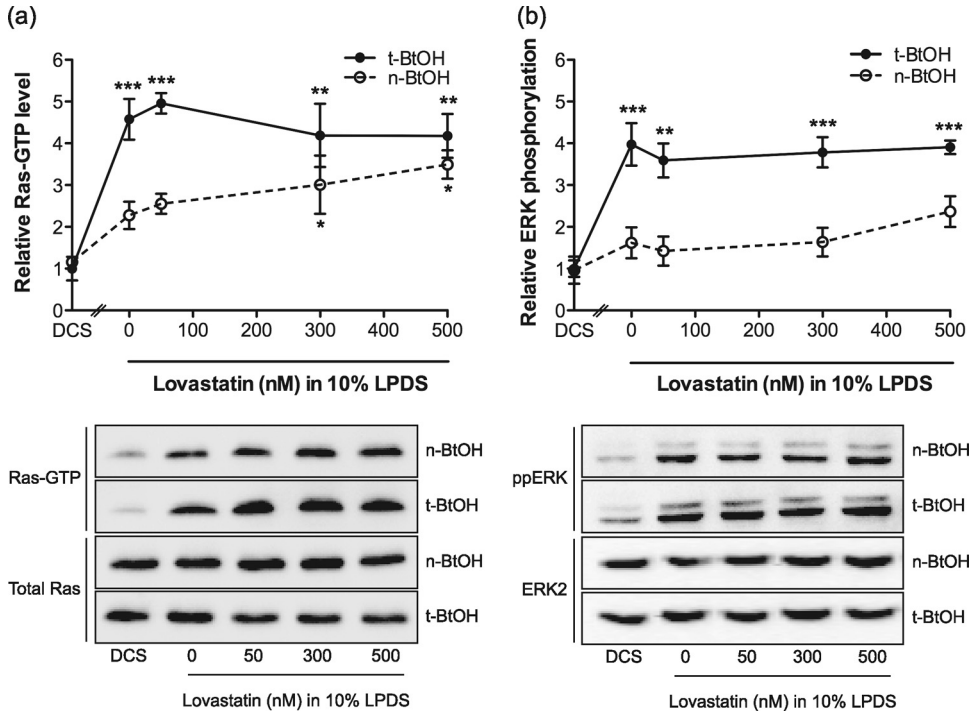

FIG. 5. PLD activity is required for Ras and ERK activation in response to cholesterol depletion. BHK cells were treated with lovastatin for 48 h in the presence of 10% LPDS. Control cells were cultured in 10% DCS. For the final 4 h of incubation, *n*-butanol (BtOH) or *t*-BtOH was added to the growth medium to give a final concentration of 1% (vol/vol). Ras-GTP levels were measured using an RBD pulldown assay (a) and ppERK levels measured by quantitative immunoblotting (b). A representative blot for each experiment is shown, with total Ras and ERK2 used as loading controls. Growth in *n*-butanol inhibits phosphatidic acid production by PLD, whereas growth in *t*-butanol does not (Materials and Methods). The graphs show mean levels ± SEM for 3 independent experiments. Differences between lovastatin-treated and control cells grown in *n*-BtOH or *t*-BtOH were assessed using one-way ANOVA tests. Significant differences are indicated (*, $P < 0.05$; **, $P < 0.01$; ***, $P < 0.001$).

tin-treated cells was completely reversed in the presence of the EGFR inhibitor, AG1478, whereas ERK activation (Fig. 7c) and Ras activation (Fig. 7e) were unaffected by AG1478. EGFR and ppERK levels in control cells grown in DCS and lovastatin were also unaffected by AG1478 (Fig. 7b and d).

To further explore the specific role of PLD2 in Ras activation mediated by lovastatin-induced cholesterol depletion, we studied the effect of ectopically expressing wild-type (WT) murine PLD2 (mPLD2) or a catalytically inactive mutant (K758R) of PLD2 that acts as a dominant interfering mutant (65). BHK cells stably expressing GFP-mPLD2 WT or GFP-mPLD2 K758R were treated with lovastatin for 48 h, and the levels of Ras-GTP and ppERK were measured. Figure 8a shows that expression of mPLD2 WT significantly enhanced, and that expression of mPLD2 K758R blocked, Ras activation in response to lovastatin treatment. These changes in Ras-GTP levels were reflected in similar effects on MAPK activation measured as ppERK (Fig. 8b). Expression of mPLD2 K758R also abrogated the inhibition of Akt induced by lovastatin but did not prevent EGFR downregulation induced by lovastatin treatment (Fig. 8c and d).

Taken together, these results suggest that cholesterol depletion by lovastatin enhances the catalytic activity of PLD2, promoting phosphatidic acid production, which leads to Ras/MAPK activation and Akt inhibition. We further conclude that activation of PLD2 leading in turn to activation of Ras and the MAPK cascade and low-level activation of the EGFR leading to downregulation of EGFR levels are likely independent effects of statin-induced cholesterol depletion.

DISCUSSION

In this report, we examined to what extent Ras prenylation is affected by therapeutic levels of lovastatin and explored more broadly the effect of statins on Ras signal transduction. We show that clinically relevant concentrations of lovastatin (50 to 500 nM), which significantly lower total cellular cholesterol levels, do not affect Ras, Rap, or Rho prenylation. Cells preferentially use farnesyl-pyrophosphate for protein prenylation over cholesterol biosynthesis, as evidenced by an 50% inhibitory concentration (IC_{50}) of 2.6 μM lovastatin for Ras farnesylation and an IC_{50} of 9.8 nM lovastatin for cholesterol biosynthesis (56). Thus, while nonphysiological, high-lovastatin concentrations (10 to 50 μM) inhibit Ras signaling by blocking farnesylation and membrane binding (27), this is not a mechanism that is likely to be clinically relevant. In contrast, we observed that cholesterol depletion induced by therapeutic levels of lovastatin enhanced Ras activation and stimulated MAPK activity. Several lines of evidence implicate PLD2 as the critical target of lovastatin action in the Ras signaling pathway: a chemical inhibitor of PLD and a dominant interfering mutant of PLD2 both blocked Ras/MAPK activation induced by lovastatin, whereas ectopic expression of wild-type PLD2 enhanced Ras/MAPK activation induced by lovastatin.

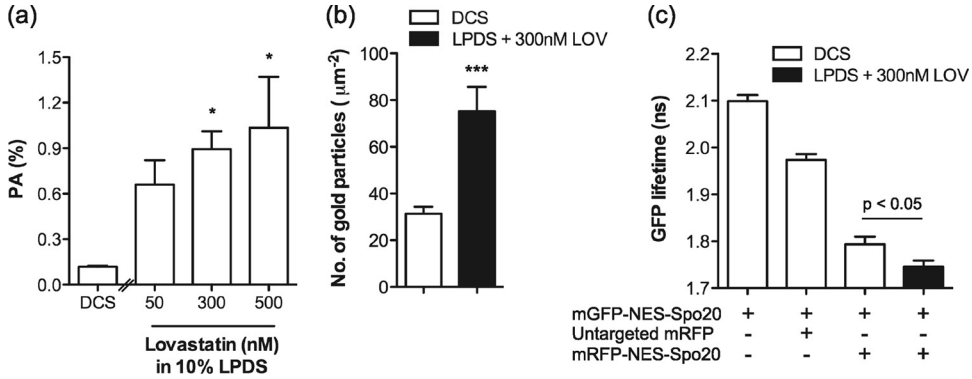

FIG. 6. Cholesterol depletion stimulates phosphatidic acid production at the plasma membrane. (a) BHK cells were treated with lovastatin for 32 h in the presence of 10% LPDS. Control cells were cultured in standard growth medium containing 10% DCS. In each case, cells were then labeled with [^{3}H]palmitate for a further 16 h. Cellular lipids were extracted and resolved by TLC. The graph shows mean phosphatidic acid (PA) level as a percentage of total phospholipids ± SEM for 3 independent experiments. Differences between lovastatin-treated and control cells were assessed using one-way ANOVA tests, and significant differences are indicated (*, $P < 0.05$). (b) Intact plasma membrane sheets were generated from BHK cells expressing mGFP-NES-Spo20 and cultured for 48 h in 300 nM lovastatin (LOV) in 10% LPDS or in normal medium containing 10% DCS. Plasma membrane sheets were labeled with anti-GFP antibody conjugated to 5-nm gold particles. The graph shows the mean number of gold particles/μm^2 (± SEM). Differences between lovastatin-treated and control cells were assessed using two-tailed *t* tests. Significant differences are indicated (***, $P < 0.001$). (c) BHK cells coexpressing mGFP-NES-Spo20 and mRFP-NES-Spo20 or mRFP were cultured in normal medium containing 10% DCS or 10% LPDS with 300 nM lovastatin for 48 h. Cells were imaged in a wide-field FLIM microscope. The graph represents the mean fluorescence lifetime of GFP (± SEM). Differences between lovastatin-treated and control cells were assessed using two-tailed *t* tests. Significant differences are indicated. BHK cells expressing mGFP-NES-Spo20 alone cultured in standard growth medium was used to determine initial mGFP lifetime. In this assay a reduction in mGFP lifetime indicates increased FRET between mGFP and mRFP.

Previous work has shown that PLD2 may be associated with cholesterol-dependent plasma membrane nanodomains, commonly called lipid rafts (10), and that cholesterol depletion leads to PLD2 activation (11). Collecting these data together with the new results presented in this paper, we propose that PLD2 is a cholesterol-sensitive regulator of the Ras/MAPK signaling pathway.

The exact mechanism by which cholesterol depletion activates PLD2 is not clear, but the subsequent molecular mechanism that leads to Ras activation has been elucidated. Activation of PLD2 remodels the lipid bilayer by hydrolyzing phosphatidylcholine to phosphatidic acid, and this drives recruitment of the Ras exchange factor Sos by direct binding of the Sos PH domain to phosphatidic acid (65). On the nanoscale, therefore, activated PLD2 will drive colocalization of plasma membrane-recruited Sos and plasma membrane-localized Ras, promoting Ras GTP loading (24). Protein- and lipid-based sorting of Ras proteins into nanoclusters on the plasma membrane is critically important for Ras signaling (28, 50, 51). Interestingly, neither K-Ras-GTP nanoclusters nor H-Ras-GTP nanoclusters to which Raf/MEK and ERK are specifically recruited from the cytosol for activation require cholesterol to form (49–52, 59). Cholesterol depletion induced by lovastatin therefore facilitates Ras GTP loading but does not impair the formation or assembly of active Ras-GTP signaling nanoclusters, resulting in increased MAPK output. Acute cholesterol depletion as a consequence of treating cells with methyl-β-cyclodextrin (MβCD) also increases ERK phosphorylation by inactivating an ERK-specific phosphatase (61). Potential differences between acute MβCD and chronic lovastatin treatment on cell signaling remain to be further investigated but indicate that cholesterol depletion regulates the Ras/MAPK pathway at multiple levels.

Statin-induced cholesterol depletion also resulted in downregulation of EGFR levels in both HUVECs and BHK cells. Furthermore, this downregulation correlated with low-level activation of the EGFR and was completely abrogated by treating statin-exposed cells with the EGFR kinase inhibitor, AG1478. Taken together, these results indicate that downregulation of EGFR levels is a direct consequence of statin-induced EGFR activation. We have shown recently that activation of PLD2 drives increased EGFR clustering but not increased EGFR activation (2). Consistent with these results, inhibition of PLD2 activity did not prevent statin-induced EGFR activation or downregulation of EGFR levels. Interestingly, blocking EGFR activity with AG1478 had minimal effect on Ras GTP loading and MAPK activation, indicating that the major input for Ras activation is through PLD2. This set of results also rationalizes the reduced pAkt levels we observed in statin-treated cells. Activation of PI3K is achieved by multiple inputs, and a major input is through activated tyrosine kinases such as the EGFR, whereas high-strength signaling from Ras-GTP is required to significantly enhance PI3K activity (21, 48). Therefore, in statin-treated cells, downregulation of the EGFR and possibly other GFRs will reduce PI3K activation and hence Akt activation, because the Ras activation induced by PLD2, while sufficient to activate Raf, is insufficient to activate PI3K.

In contrast to our results, lovastatin was reported to inhibit EGF-induced EGFR autophosphorylation; however, this required very high doses (10 μM) that would be expected to inhibit Rho and Ras prenylation (41). Previous studies have shown variable effects of statin treatment on MAPK activation, ranging from stimulation (9, 14, 62) to inhibition (5, 7, 47). One possible explanation of these diverse results is that cholesterol depletion by statins has different effects depending on cell type and experimental conditions (e.g., statin concentration, incubation time, and/or serum starvation/stimulation). Indeed, we have also observed that caveolin-1 expression is differentially

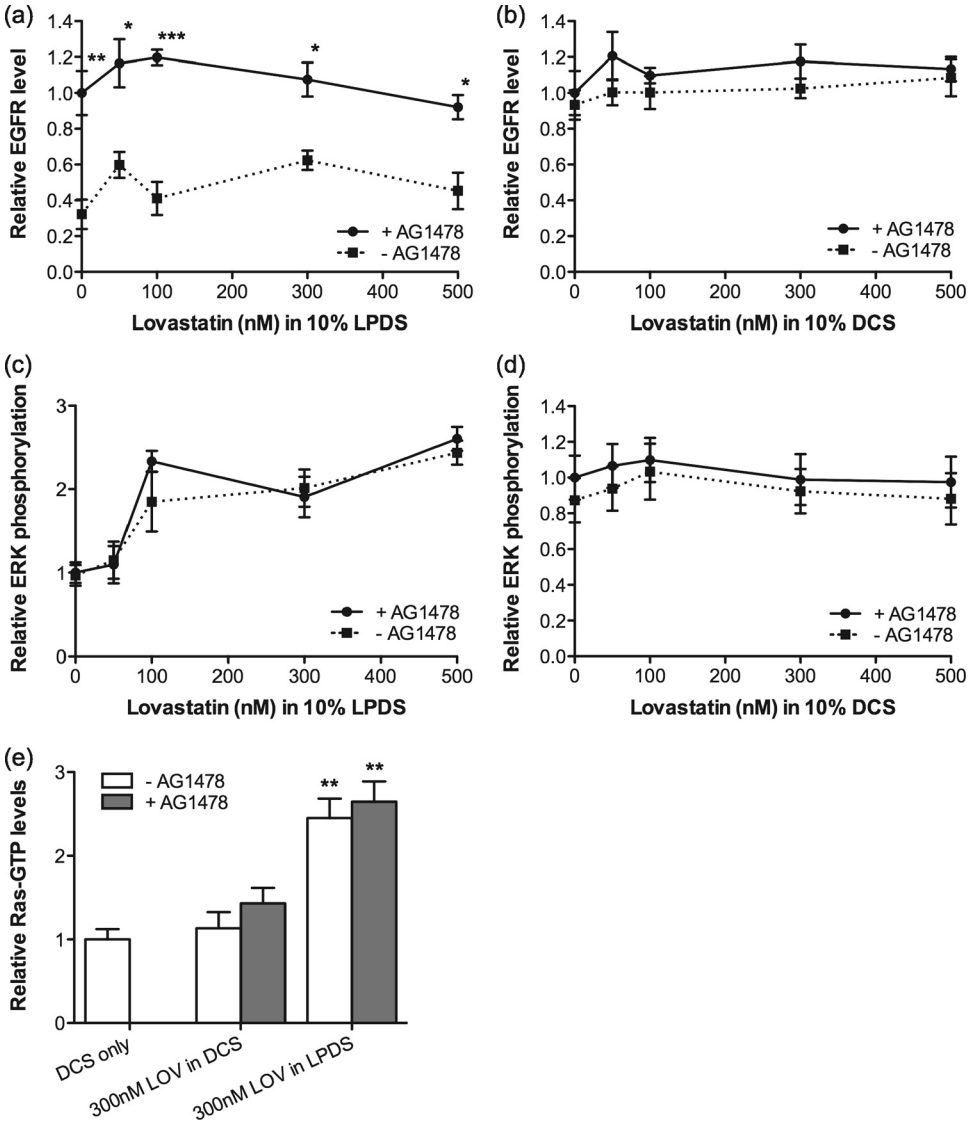

FIG. 7. Lovastatin-induced EGFR downregulation is blocked by EGFR inhibition. BHK cells were cultured for 48 h in normal medium containing 10% DCS or 10% LPDS in the presence of lovastatin with or without 0.5 μM AG1478. Cell lysates were assayed for total EGFR (a and b) or ppERK (c and d). The graphs show mean levels of total EGFR or ppERK, relative to levels in AG1478-treated cells grown with lovastatin under each culture condition, ± SEM for 3 independent experiments. Differences between AG1478-untreated and AG1478-treated cells at each lovastatin concentration were assessed using two-tailed *t* tests. Significant differences are indicated (*, $P < 0.05$; **, $P < 0.01$; ***, $P < 0.001$). (e) BHK cells were cultured for 48 h in 10% LPDS plus 300 nM lovastatin or 10% DCS plus 300 nM lovastatin with or without 0.5 μM AG1478. These growth conditions replicate those represented in Fig. 1a, where the presence of DCS maintains normal cell cholesterol levels in the presence of lovastatin. Control cells were cultured in standard growth medium containing 10% DCS. Total Ras-GTP levels were measured. The graphs show means ± SEM of results from 3 independent experiments. Differences between lovastatin-treated and control cells were assessed using one-way ANOVA tests. Significant differences are indicated (**, $P < 0.01$).

regulated in HUVECs and BHK cells in response to cholesterol depletion by lovastatin (K.-J. Cho, unpublished data).

What mechanistic insights into the clinical benefits of statin treatment flow from these data? ERK activation directly stimulates NO production in many cell lines, including endothelium (8, 19, 64). Therefore, a direct consequence of statin-induced activation of the PLD2/Ras/MAPK signaling pathway may be improved endothelial function by increased synthesis of NO (36). In addition, the lovastatin-induced reduction in caveolin-1 levels that we have observed in endothelial cells would be expected to further increase endothelial NO synthesis, since caveolin-1 is a negative regulator of endothelial NO synthase (eNOS) (18, 44). The Ras/MAPK signal pathway also regulates expression of bone morphogenetic protein 2 (BMP-2), which promotes atherosclerotic plaque stability (13, 14, 58).

Our focus throughout this study has been on the ability of statins to reduce cellular cholesterol levels by a combination of reduction of LDL-C levels and a direct effect on cellular cholesterol synthesis. It is also clear from Fig. 1 and 2 that the major effect on cellular cholesterol is mediated at the level of reduced LDL-C. Very few clinical studies have rigorously examined cellular cholesterol levels in patients treated with

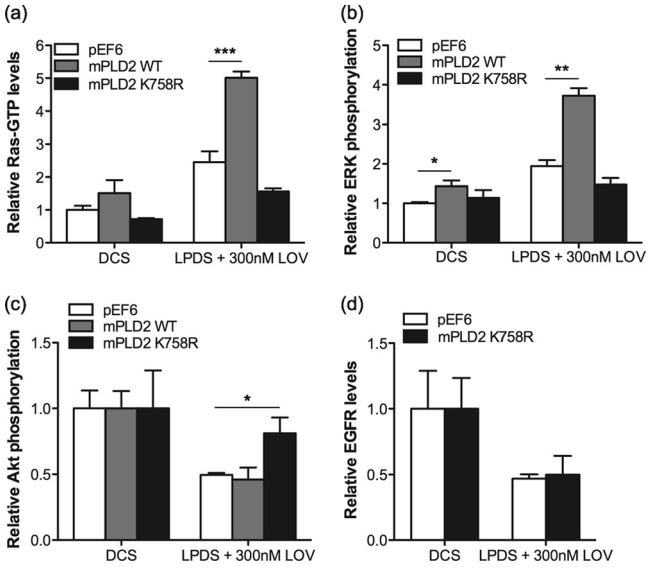

FIG. 8. Lovastatin-induced activation of PLD2 and EGFR are independent events. BHK cells stably expressing GFP-mPLD2 WT, GFP-mPLD2 K758R, or empty pEF6 vector were treated with 300 nM lovastatin for 48 h. Control cells were cultured in standard growth medium containing 10% DCS. Ras-GTP (a) ppERK (b) and pAkt (S473) (c) levels were measured by quantitative immunoblotting. The graphs show mean values ± SEM for 3 independent experiments. The effect of ectopic expression of mPLD2 WT or mPLD2 K758R with lovastatin against pEF6 was assessed using one-way ANOVA tests. Significant differences are indicated (*, $P < 0.05$; **, $P < 0.01$; ***, $P < 0.001$). (d) BHK cells stably expressing GFP-mPLD2 K758R or empty pEF6 vector were treated for 48 h with lovastatin in 10% LPDS. Cell lysates were assayed for total EGFR by quantitative immunoblotting. The graphs show means ± SEM for 3 independent experiments. No significant difference in EGFR levels between pEF6-transfected and GFP-mPLD2 K758R-expressing cells were detected using two-tailed *t* tests.

statins; however, there are reports of significantly reduced erythrocyte and platelet cholesterol levels in statin-treated patients (32, 40). In these studies, the extent of cellular cholesterol depletion was similar to that achieved in our model *in vitro* system.

In summary, our results demonstrate that while therapeutic levels of lovastatin do not inhibit protein prenylation, cholesterol depletion induced by lovastatin promotes activities of PLD2, Ras, and MAPK by possible perturbation of cholesterol-sensitive nanodomains. Thus, our study strongly suggests that modulation of cholesterol-dependent membrane organization plays a major role in statin action and that certain pleiotropic "cholesterol-independent" effects of statins are, in fact, on target cholesterol-dependent effects.

ACKNOWLEDGMENTS

We thank Mike Frohman for the PLD2 constructs and Sarah Plowman for helpful advice.

This work was supported by grants from the National Health and Medical Research Council, Australia, and NIH GM066717 and GM071475. J.F.H. is the present incumbent of the Fondren Chair in Cellular Signaling. M.M.H. is supported by a Career Development Fellowship (no. 569512) from the National Health and Medical Research Council, Australia.

REFERENCES

1. **Adamson, P., H. F. Paterson, and A. Hall.** 1992. Intracellular localization of the P21rho proteins. J. Cell Biol. **119:**617–627.
2. **Ariotti, N., et al.** 2010. Epidermal growth factor receptor activation remodels the plasma membrane lipid environment to induce nanocluster formation. Mol. Cell. Biol. **30:**3795–3804.
3. **Arnaud, C., V. Braunersreuther, and F. Mach.** 2005. Toward immunomodulatory and anti-inflammatory properties of statins. Trends Cardiovasc. Med. **15:**202–206.
4. **Berzat, A. C., D. C. Brady, J. J. Fiordalisi, and A. D. Cox.** 2006. Using inhibitors of prenylation to block localization and transforming activity. Methods Enzymol. **407:**575–597.
5. **Campbell, M. J., et al.** 2006. Breast cancer growth prevention by statins. Cancer Res. **66:**8707–8714.
6. **Casey, P. J., P. A. Solski, C. J. Der, and J. E. Buss.** 1989. p21ras is modified by a farnesyl isoprenoid. Proc. Natl. Acad. Sci. U. S. A. **86:**8323–8327.
7. **Cerezo-Guisado, M. I., et al.** 2007. Lovastatin inhibits the extracellular-signal-regulated kinase pathway in immortalized rat brain neuroblasts. Biochem. J. **401:**175–183.
8. **Cha, M. S., M. J. Lee, G. H. Je, and J. Y. Kwak.** 2001. Endogenous production of nitric oxide by vascular endothelial growth factor down-regulates proliferation of choriocarcinoma cells. Biochem. Biophys. Res. Commun. **282:**1061–1066.
9. **Chen, J. C., M. L. Wu, K. C. Huang, and W. W. Lin.** 2008. HMG-CoA reductase inhibitors activate the unfolded protein response and induce cytoprotective GRP78 expression. Cardiovasc. Res. **80:**138–150.
10. **Cho, C. H., et al.** 2004. Localization of VEGFR-2 and PLD2 in endothelial caveolae is involved in VEGF-induced phosphorylation of MEK and ERK. Am. J. Physiol. Heart Circ. Physiol. **286:**H1881–H1888.
11. **Diaz, O., et al.** 2005. Disruption of lipid rafts stimulates phospholipase d activity in human lymphocytes: implication in the regulation of immune function. J. Immunol. **175:**8077–8086.
12. **Eisenberg, S., D. E. Shvartsman, M. Ehrlich, and Y. I. Henis.** 2006. Clustering of raft-associated proteins in the external membrane leaflet modulates internal leaflet h-ras diffusion and signaling. Mol. Cell. Biol. **26:**7190–7200.
13. **Emmanuele, L., J. Ortmann, T. Doerflinger, T. Traupe, and M. Barton.** 2003. Lovastatin stimulates human vascular smooth muscle cell expression of bone morphogenetic protein-2, a potent inhibitor of low-density lipoprotein-stimulated cell growth. Biochem. Biophys. Res. Commun. **302:**67–72.
14. **Ghosh-Choudhury, N., C. C. Mandal, and G. G. Choudhury.** 2007. Statin-induced Ras activation integrates the phosphatidylinositol 3-kinase signal to Akt and MAPK for bone morphogenetic protein-2 expression in osteoblast differentiation. J. Biol. Chem. **282:**4983–4993.
15. **Goldstein, J. L., and M. S. Brown.** 1990. Regulation of the mevalonate pathway. Nature **343:**425–430.
16. **Graaf, M. R., A. B. Beiderbeck, A. C. Egberts, D. J. Richel, and H. J. Guchelaar.** 2004. The risk of cancer in users of statins. J. Clin. Oncol. **22:**2388–2394.
17. **Graaf, M. R., D. J. Richel, C. J. van Noorden, and H. J. Guchelaar.** 2004. Effects of statins and farnesyltransferase inhibitors on the development and progression of cancer. Cancer Treat. Rev. **30:**609–641.
18. **Gratton, J. P., et al.** 2000. Reconstitution of an endothelial nitric-oxide synthase (eNOS), hsp90, and caveolin-1 complex in vitro. Evidence that hsp90 facilitates calmodulin stimulated displacement of eNOS from caveolin-1. J. Biol. Chem. **275:**22268–22272.
19. **Grossini, E., C. Molinari, P. P. Caimmi, F. Uberti, and G. Vacca.** 2009. Levosimendan induces NO production through p38 MAPK, ERK and Akt in porcine coronary endothelial cells: role for mitochondrial K(ATP) channel. Br. J. Pharmacol. **156:**250–261.
20. **Grundy, S. M., et al.** 2004. Implications of recent clinical trials for the National Cholesterol Education Program Adult Treatment Panel III guidelines. Circulation **110:**227–239.
21. **Gupta, S., et al.** 2007. Binding of ras to phosphoinositide 3-kinase p110alpha is required for ras-driven tumorigenesis in mice. Cell **129:**957–968.
22. **Gutierrez, L., A. I. Magee, C. J. Marshall, and J. F. Hancock.** 1989. Post-translational processing of p21ras is two-step and involves carboxyl-methylation and carboxy-terminal proteolysis. EMBO J. **8:**1093–1098.
23. **Hancock, J. F.** 2006. Lipid rafts: contentious only from simplistic standpoints. Nat. Rev. Mol. Cell Biol. **7:**456–462.
24. **Hancock, J. F.** 2007. PA promoted to manager. Nat. Cell Biol. **9:**615–617.
25. **Hancock, J. F.** 1995. Prenylation and palmitoylation analysis. Methods Enzymol. **255:**237–245.
26. **Hancock, J. F.** 2003. Ras proteins: different signals from different locations. Nat. Rev. Mol. Cell Biol. **4:**373–384.
27. **Hancock, J. F., A. I. Magee, J. E. Childs, and C. J. Marshall.** 1989. All ras proteins are polyisoprenylated but only some are palmitoylated. Cell **57:**1167–1177.
28. **Hancock, J. F., and R. G. Parton.** 2005. Ras plasma membrane signalling platforms. Biochem. J. **389:**1–11.
29. **Hancock, J. F., H. Paterson, and C. J. Marshall.** 1990. A polybasic domain

or palmitoylation is required in addition to the CAAX motif to localize p21ras to the plasma membrane. Cell **63:**133–139.
30. **Harding, A. S., and J. F. Hancock.** 2008. Using plasma membrane nanoclusters to build better signaling circuits. Trends Cell Biol. **18:**364–371.
31. **Heasman, S. J., and A. J. Ridley.** 2008. Mammalian Rho GTPases: new insights into their functions from in vivo studies. Nat. Rev. Mol. Cell Biol. **9:**690–701.
32. **Hochgraf, E., Y. Levy, M. Aviram, J. G. Brook, and U. Cogan.** 1994. Lovastatin decreases plasma and platelet cholesterol levels and normalizes elevated platelet fluidity and aggregation in hypercholesterolemic patients. Metabolism **43:**11–17.
33. **Honda, A., et al.** 1999. Phosphatidylinositol 4-phosphate 5-kinase alpha is a downstream effector of the small G protein ARF6 in membrane ruffle formation. Cell **99:**521–532.
34. **Jenkins, G. M., and M. A. Frohman.** 2005. Phospholipase D: a lipid centric review. Cell. Mol. Life Sci. **62:**2305–2316.
35. **Kita, T., M. S. Brown, and J. L. Goldstein.** 1980. Feedback regulation of 3-hydroxy-3-methylglutaryl coenzyme A reductase in livers of mice treated with mevinolin, a competitive inhibitor of the reductase. J. Clin. Invest. **66:**1094–1100.
36. **Laufs, U.** 2003. Beyond lipid-lowering: effects of statins on endothelial nitric oxide. Eur. J. Clin. Pharmacol. **58:**719–731.
37. **Laufs, U., and J. K. Liao.** 1998. Post-transcriptional regulation of endothelial nitric oxide synthase mRNA stability by Rho GTPase. J. Biol. Chem. **273:** 24266–24271.
38. **Lewis, K. A., S. A. Holstein, and R. J. Hohl.** 2005. Lovastatin alters the isoprenoid biosynthetic pathway in acute myelogenous leukemia cells in vivo. Leuk. Res. **29:**527–533.
39. **Liao, J. K., and U. Laufs.** 2005. Pleiotropic effects of statins. Annu. Rev. Pharmacol. Toxicol. **45:**89–118.
40. **Lijnen, P., H. Celis, R. Fagard, J. Staessen, and A. Amery.** 1994. Influence of cholesterol lowering on plasma membrane lipids and cationic transport systems. J. Hypertens. **12:**59–64.
41. **Mantha, A. J., et al.** 2005. Targeting the mevalonate pathway inhibits the function of the epidermal growth factor receptor. Clin. Cancer Res. **11:**2398–2407.
42. **Mason, R. P., M. F. Walter, and R. F. Jacob.** 2004. Effects of HMG-CoA reductase inhibitors on endothelial function: role of microdomains and oxidative stress. Circulation **109:**II34–41.
43. **Michaelson, D., et al.** 2001. Differential localization of Rho GTPases in live cells: regulation by hypervariable regions and RhoGDI binding. J. Cell Biol. **152:**111–126.
44. **Michel, J. B., O. Feron, D. Sacks, and T. Michel.** 1997. Reciprocal regulation of endothelial nitric-oxide synthase by Ca2+-calmodulin and caveolin. J. Biol. Chem. **272:**15583–15586.
45. **Mor, A., et al.** 2007. The lymphocyte function-associated antigen-1 receptor costimulates plasma membrane Ras via phospholipase D2. Nat. Cell Biol. **9:**713–719.
46. **Niv, H., O. Gutman, Y. Kloog, and Y. I. Henis.** 2002. Activated K-Ras and H-Ras display different interactions with saturable nonraft sites at the surface of live cells. J. Cell Biol. **157:**865–872.
47. **Ogunwobi, O. O., and I. L. Beales.** 2008. Statins inhibit proliferation and induce apoptosis in Barrett's esophageal adenocarcinoma cells. Am. J. Gastroenterol. **103:**825–837.
48. **Orme, M. H., S. Alrubaie, G. L. Bradley, C. D. Walker, and S. J. Leevers.** 2006. Input from Ras is required for maximal PI(3)K signalling in Drosophila. Nat. Cell Biol. **8:**1298–1302.
49. **Plowman, S. J., N. Ariotti, A. Goodall, R. G. Parton, and J. F. Hancock.** 2008. Electrostatic interactions positively regulate K-Ras nanocluster formation and function. Mol. Cell. Biol. **28:**4377–4385.
50. **Plowman, S. J., C. Muncke, R. G. Parton, and J. F. Hancock.** 2005. H-ras, K-ras, and inner plasma membrane raft proteins operate in nanoclusters with differential dependence on the actin cytoskeleton. Proc. Natl. Acad. Sci. U. S. A. **102:**15500–15505.
51. **Prior, I. A., et al.** 2001. GTP-dependent segregation of H-ras from lipid rafts is required for biological activity. Nat. Cell Biol. **3:**368–375.
52. **Prior, I. A., C. Muncke, R. G. Parton, and J. F. Hancock.** 2003. Direct visualization of Ras proteins in spatially distinct cell surface microdomains. J. Cell Biol. **160:**165–170.
53. **Rikitake, Y., and J. K. Liao.** 2005. Rho GTPases, statins, and nitric oxide. Circ. Res. **97:**1232–1235.
54. **Roy, S., et al.** 1999. Dominant-negative caveolin inhibits H-Ras function by disrupting cholesterol-rich plasma membrane domains. Nat. Cell Biol. **1:**98–105.
55. **Simons, K., and D. Toomre.** 2000. Lipid rafts and signal transduction. Nat. Rev. Mol. Cell Biol. **1:**31–39.
56. **Sinensky, M., L. A. Beck, S. Leonard, and R. Evans.** 1990. Differential inhibitory effects of lovastatin on protein isoprenylation and sterol synthesis. J. Biol. Chem. **265:**19937–19941.
57. **Smith, S. C., Jr., et al.** 2006. AHA/ACC guidelines for secondary prevention for patients with coronary and other atherosclerotic vascular disease: 2006 update: endorsed by the National Heart, Lung, and Blood Institute. Circulation **113:**2363–2372.
58. **Sukhova, G. K., J. K. Williams, and P. Libby.** 2002. Statins reduce inflammation in atheroma of nonhuman primates independent of effects on serum cholesterol. Arterioscler. Thromb. Vasc. Biol. **22:**1452–1458.
59. **Tian, T., et al.** 2007. Plasma membrane nanoswitches generate high-fidelity Ras signal transduction. Nat. Cell Biol. **9:**905–914.
60. **Vaughan, C. J., and A. M. Gotto, Jr.** 2004. Update on statins: 2003. Circulation **110:**886–892.
61. **Wang, P. Y., J. Weng, and R. G. Anderson.** 2005. OSBP is a cholesterol-regulated scaffolding protein in control of ERK 1/2 activation. Science **307:** 1472–1476.
62. **Yano, M., et al.** 2007. Statins activate peroxisome proliferator-activated receptor gamma through extracellular signal-regulated kinase 1/2 and p38 mitogen-activated protein kinase-dependent cyclooxygenase-2 expression in macrophages. Circ. Res. **100:**1442–1451.
63. **Yeo, E. J., and J. H. Exton.** 1995. Stimulation of phospholipase D by epidermal growth factor requires protein kinase C activation in Swiss 3T3 cells. J. Biol. Chem. **270:**3980–3988.
64. **Yuan, Z., et al.** 2009. p38MAPK and ERK promote nitric oxide production in cultured human retinal pigmented epithelial cells induced by high concentration glucose. Nitric Oxide **20:**9–15.
65. **Zhao, C., G. Du, K. Skowronek, M. A. Frohman, and D. Bar-Sagi.** 2007. Phospholipase D2-generated phosphatidic acid couples EGFR stimulation to Ras activation by Sos. Nat. Cell Biol. **9:**706–712.